Control of Surface Chemical Structure and Functional Property of Langmuir-Blodgett Film Composed of New Polymerizable Amphiphile with a Sodium Sulfonate

Motoko Uchida, Tatsuya Tanizaki, Takashi Oda,† and Tisato Kajiyama*

Department of Applied Chemistry, Faculty of Engineering, Kyushu University, Fukuoka 812, Japan

Received August 31, 1990; Revised Manuscript Received January 3, 1991

ABSTRACT: A new amphiphile with a sodium sulfonate and two polymerizable alkyl chains, sodium 1,2-bis[[[16-(acryloyloxy)hexadecyl]oxy]carbonyl]ethane-1-sulfonate ($2AC_{16}SNa$), was synthesized. $2AC_{16}SNa$ monolayer on a pure water surface was composed of two-dimensional crystalline domains and became morphologically homogeneous by compressing it up to 35 $mN \cdot m^{-1}$. $2AC_{16}ANa$ Langmuir-Blodgett (LB) film transferred to a polystyrene film by Langmuir-Blodgett techniques at the built-up pressure of 35 $mN \cdot m^{-1}$ had a bilayer lamella structure with a high degree of lamella-plane orientation. The monomeric LB film was polymerized to stabilize the surface chemical structure (hydrophilicity or hydrophobicity). The highly oriented bilayer lamella structure was retained even after polymerization. The hydrophilic and hydrophobic surfaces of the LB film were immobilized by polymerizations carried out in water and in air, respectively. This is due to the progression of interlayer and/or intramonolayer polymerizations in the LB film, resulting in the restriction of overturning of the outermost monolayer. The blood compatibility of the LB film composed of $2Ac_{16}SNa$ was investigated on the basis of the interaction with human blood platelets. The polymerized LB film with a sulfonic group orienting normal to the LB film surface showed an excellent blood compatibility, mainly owing to its negatively charged surface which repelled platelets.

Introduction

Special attention has been focused on the development of biomedical artificial materials. For artificial materials such as a diaphragm of a blood pump for artificial heart systems, excellent blood compatibility (surface property) and mechanical strength (bulk property) are required. It has been reported that segmented poly(urethane-urea) has good blood compatibility and mechanical properties owing to its microphase separated structure composed of hard- and soft-segment domains.[1-5] However, the surface property of polymers including segmented poly(urethane-urea)s is often different from the bulk one and changes depending on the environment.[6] It is difficult to design the molecular structure of a biomedical polymer with both optimum bulk and stable surface properties. To get around this problem, surface modification and surface stabilization of materials with optimum mechanical bulk properties are useful.[7]

It is known that the internal surfaces of natural blood vessels are negatively charged owing to the existence of sulfate and carboxylate groups at their surfaces. This negatively charged surface electrostatically repels blood components, such as platelets, which are also negatively charged and ensures the blood compatibility of natural blood vessel.[8] The Langmuir-Blodgett (LB) method[9] is suitable for surface modification to obtain the negatively charged surface without any change of the mechanical bulk properties of materials.[10]

LB films prepared from amphiphiles are organic ultrathin films with highly ordered layer structures. The surface chemical structure (hydrophilicity or hydrophobicity) of LB films is easily designed by orienting the hydrophilic part or the hydrophobic part of an amphiphile on the film surface. However, the surface chemical structure of LB films may be very unstable and depends on the environmental conditions (in water or in air). The hydrophobic parts of the amphiphiles at the outermost monolayer orient to the film surface, as when a LB film is exposed to air, and the hydrophilic parts orient to the film surface, as when a LB film is dipped in water, to minimize the interfacial free energy between the surface of the LB film and the environment.

On the other hand, we have reported that the surface chemical structure of the LB film composed of the amphiphile with a polymerizable group in its hydrophobic part was stabilized by polymerization.[11] Figure 1 shows the schematic representation of the surface structure being stabilized by means of polymerization of a LB film composed of polymerizable amphiphile. In Figure 1A, the monomeric LB film orienting the hydrophobic part to the film surface is polymerized in air to stabilize the hydrophobic surface. This is type I film. The hydrophobic surface of the polymerized LB film can be stable even in the water, because the widely polymerized domain in the outermost monolayer can hardly turn over compared with the monomeric film. In Figure 1B, the monomeric LB film orienting the hydrophilic part to the film surface is polymerized in water to stabilize the hydrophilic surface. This is type II film. The hydrophilic surface of the polymerized LB film can be maintained even in air, because the interlayer polymerization is supposed to occur. When interlayer polymerization occurs, the neighboring monolayers are chemically bonded and the outermost polymerized monolayer can hardly be rearranged individually. Therefore, the surface modification of material by the LB method using the amphiphile with polymerizable hydrophobic parts can be effective.

In this study, to obtain a blood compatible material, the surface modification of material by the LB method using the amphiphile with a sulfonate and the polymerizable hydrophobic part was investigated.

Experimental Section

Materials. Figure 2 shows the chemical structure and the synthetic route of the polymerizable amphiphile with the sodium sulfonate, sodium 1,2-bis[[[16-(acryloyloxy)hexadecyl]oxy]carbonyl]ethane-1-sulfonate ($2AC_{16}SNa$). At each synthetic step,

* To whom correspondence should be addressed.
† On leave from Kao Co. Ltd., Wakayama 640, Japan.

0024-9297/91/2224-3238$02.50/0

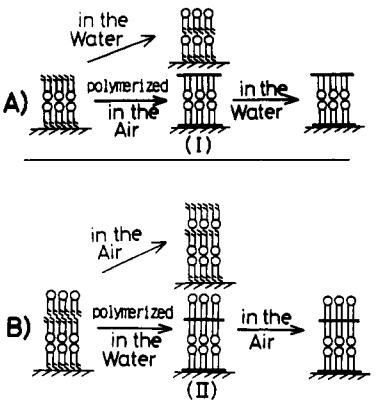

Figure 1. Schematic representations of the surface structure being stabilized by means of polymerization of LB film composed of polymerizable amphiphile.

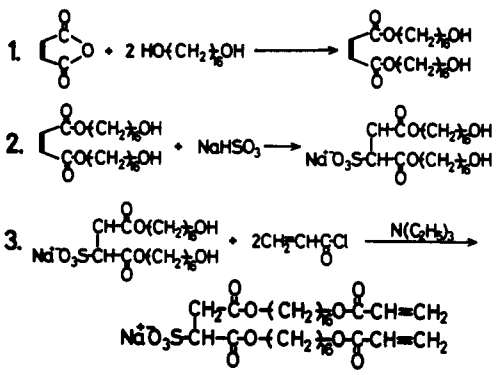

Figure 2. Chemical structure and synthetic route of $2AC_{16}SNa$.

the products were analyzed by IR (Hitachi 270-30 spectrophotometer), ^1H and ^{13}C NMR (JEOL GX-400, 400 MHz), mass spectroscopy (Hitachi M-80 mass spectrometer), and thin-layer chromatography (TLC) (Kieselgel 60, Article 11845, Merck).

1,16-Hexadecanediol (42.2 g, 0.16 mol) and maleic anhydride (4.0 g, 0.041 mol) were added to 30 mL of dry toluene at 373 K. After 3 h, a few drops of concentrated H_2SO_4 were added, and azeotropic water was removed for 3 h. The solvent was then removed. The residue was dissolved in chloroform and purified by gel permeation chromatography (Nihon Bunseki Model LC-08) to give 1 (5.5 g, 23% yield) as a white solid [mp 336 K, R_f 0.25 (benzene/isopropyl alcohol = 80/20)]. 1 (4.2 g, 7.0 mmol) and $NaHSO_3$ (3.6 g, 35 mmol) were dissolved in 10 mL of water and allowed to react at 373 K for 2 h. Water was removed in vacuo, and the residue was dissolved in a large amount of hot methanol to separate inorganic materials. Then, the solvent was removed, and the residue was recrystallized from methanol to give 2 (4.5 g, 92% yield) as white granules [mp 372 K, R_f 0.41 (benzene/methanol = 70/30)]. 2 (3.5 g, 5.0 mmol), triethylamine (4.0 g, 40 mmol), and a small amount of di-*tert*-butyl-*p*-cresol as an inhibitor were added to a 65 mL of dry dimethylformamide. To this mixture was added dropwise 2.3 g (25 mmol) of acrylic chloride at 283 K. After 40 h at room temperature, the solvent was removed in vacuo. The residue was dissolved in chloroform, washed three times with saturated aqueous NaCl, and dried. After removal of chloroform, the residue was purified by preparative TLC (Kieselgel 60 F_{254}, Article 5717, Merck) using a chloroform/methanol (80/20) mixture. Recrystallization from ether solution gave $2AC_{16}SNa$ (0.53 g, 22% yield) as white granules. The overall yield in three steps was 4.7%. $2AC_{16}SNa$: mp 353 K: R_f 0.61 (benzene/methanol = 70/30); IR (KBr) $\nu_{C=O}$ 1725, ν_{C-O-C} 1280, $\nu_{S=O}$, ν_{C-O-C} 1210, $\nu_{S=O}$ 1050, $\nu_{C=C}$ 1640, $\delta_{IP}^{CH_2}$ C=C—H 1420, $\delta_{OP}^{CH_2}$ C=C—H 980, $\delta_{OP}^{CH_2}$ C=C—H 803 cm^{-1}; ^1H NMR ($CDCl_3$) δ 1.3 (s, 48 H), 1.5–1.7 (m, 8 H), 3.1–3.2 (m, 2 H), 4.0 (T, 2 H), 4.1 (t, 6 H), 3.0 (t, 1 H), 5.8–6.4 (m, 6 H); ^{13}C NMR ($CDCl_3$) δ 171.7, 169.8, 166.3, 130.4, 128.7, 66.6, 65.3, 64.7, 61.1, 33.3, 29.9, 29.3, 28.7, 28.4, 26.0, 25.9; MS; *m/e*, 831 (M^+ + Na). Anal. Calcd for $C_{42}H_{73}O_{11}SNa \cdot 0.27H_2O$: C, 61.96; H, 9.12. Found: C, 61.96; H, 9.12.

Aggregation Structure of the Monomeric $2AC_{16}SNa$ Monolayer. The surface pressure–area (Π–A) isotherm was obtained by using a microprocessor-controlled film balance (Sanesu Keisoku Co. Ltd. FSD-25). A benzene/ethanol (4/1 v/v) solution of $2AC_{16}SNa$ with the concentration 0.1 $mg \cdot mL^{-1}$ was spread on the pure water surface at 293 K. The subphase water was purified by using a MilliQ-II (Millipore). For transmission electron microscopic (TEM) observations of monolayer, the monolayer was transferred onto Formvar-covered copper grids (200-mesh)[12] with a hydrophilic surface by the vertical dipping method[9] at surface pressures of 18, 25, and 35 $mN \cdot m^{-1}$ or by the horizontal lifting method[13] at a surface pressure of 7 $mN \cdot m^{-1}$. In the case of the vertical dipping at 18, 25, and 35 $mN \cdot m^{-1}$, the monolayer was transferred only in an upward drawing. The aggregation structure of $2AC_{16}SNa$ monolayer was studied by using a Hitachi H-500 transmission electron microscope at 75 kV and a beam current of 2.5 μA. For the bright field image observations, the samples were shadowed with platinum–carbon pellets at an angle of 23°.

Aggregation Structure of the Monomeric $2AC_{16}SNa$ LB Film. $2AC_{16}SNa$ monolayers were built up on the polystyrene film successively by the vertical dipping method at surface pressures of 18, 25, and 35 $mN \cdot m^{-1}$. The polystyrene film of 20-μm thickness was cast from a toluene solution. The aggregation structure of $2AC_{16}SNa$ LB film was studied by X-ray diffraction measurements. The X-ray diffraction patterns of the LB films were taken by using a plate camera collimated with toroid mirror optics. The incident X-ray beam was generated with Cu Kα radiation filtered by a nickel foil from a stabilized generator (Rigaku Rotaflex RU-200). Diffraction intensities were measured on a Rigaku four-circle diffractometer.

Photopolymerization of the $2AC_{16}SNa$ LB Film. $2AC_{16}SNa$ monomeric LB films were prepared on polyethylene film (commercial film) and polymerized by UV irradiation with a 500-W mercury lamp (Ushio Denki Co.) for 40 min at 303 K, which is below the crystal–liquid crystal phase transition temperature (325 K) of the monomeric LB film. The completion of the polymerization reaction was confirmed by ATR-FT-IR measurements (Nihon Bunkougaku Co. Ltd.). The aggregation structure of polymerized LB film was studied by X-ray diffraction measurements.

Surface Chemical Structure and Blood Compatibility of LB Film. The surface chemical structure of the LB film in dried atmosphere was characterized by X-ray photoelectron spectroscopy with a Shimadzu ESCA 750. The X-ray source was Mg Kα, which was obtained at 8 kV and 30 mA. The surface chemical structure of the LB films in water was characterized by contact angle measurements, which were carried out in water with air bubbles.[14] The blood compatibility of the LB film was evaluated from the degree of interaction between human blood platelets and the surfaces of LB films.[3] The film was immersed in a human platelet rich plasma (PRP) at 310 K for 1 h. The number of adhered and deformed platelets was determined by scanning electron microscopic (SEM) observation (Hitachi S-430).

Results and Discussion

Aggregation Structure of the Monomeric $2AC_{16}SNa$ Monolayer. Figure 3 shows the surface pressure–area (Π–A) isotherm of $2AC_{16}SNa$ monolayer and the bright field micrographs and electron diffraction (ED) patterns at surface pressures of 7, 18, 25, and 35 $mN \cdot m^{-1}$, respectively, at the subphase temperature of 293 K. The monolayer at the air–water interface could be transferred without changing its aggregation structure onto the hydrophilic substrate by the upward drawing method.[15] ED patterns were obtained from a monolayer area several micrometers in diameter, which corresponded with the size of the electron beam. From the point of view of the general concept of the Π–A isotherm, a liquid expanded monolayer state at very low surface pressure converted into the coexistence of liquid expanded and condensed states, the liquid condensed state, and, finally, the solid condensed state with an increase of surface pressure. However, even

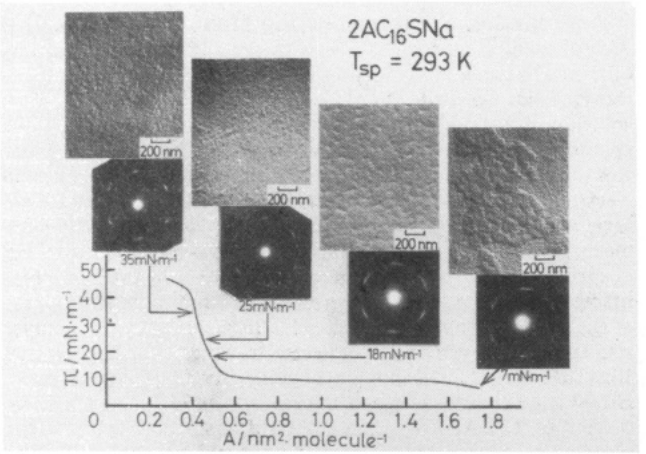

Figure 3. Π–A isotherm, bright field micrographs, and electron diffraction patterns of $2AC_{16}SNa$ monolayer film at the subphase temperature of 293 K.

at 7 mN·m^{-1}, the bright field image and ED pattern of the monolayer indicated an island structure and six crystalline spots broadened along an azimuthal direction with spacings of 0.39 and 0.42 nm, respectively. From a shadow length of the bright field image, the average thickness of isolated domains was estimated to be 3 nm, which almost corresponded to the molecular length of $2AC_{16}SNa$ calculated on the basis of a CPK molecular model. These results indicate that the two-dimensional crystallites are formed at the air–water interface, even in the case of a low surface pressure. With increasing surface pressure, the bright field images clarified the aggregating process of isolated domains and the ED patterns showed six crystalline spots that became narrower along an azimuthal direction without any change of the value of spacings. At a surface pressure of 35 mN·m^{-1}, the bright field image and ED pattern showed that a homogeneous monolayer structure with sharp crystalline spots was formed. These results indicate that the two-dimensional crystallites are gathered and orient their crystallographic directions during the compression of monolayer. Therefore, the new concept of the Π–A isotherm can be proposed on the basis of the results of Figure 3. That is, the Π–A behavior at the air–water interface does not show the phase transformation but the gathering process of two-dimensional crystalline domains which are formed right after a solution is spread at the low surface pressure on the water surface. This new concept has been proposed on the basis of polarizing and transmission microscopic observations of diacetylene fatty acid monolayer,[16] synchrotron X-ray diffraction measurements of fatty acid monolayers,[17,18] and transmission electron microscopic observations of fatty acid monolayers.[19–22] In particular, the phase of fatty acid monolayers (crystalline or amorphous phase) is strongly related to the relation between the melting temperature of monolayer on the water surface and the subphase temperature, irrespective of surface pressure.[21,22] At present, it is not clear why the crystallographic orientation of crystalline domains becomes fairly aligned by surface compression, but fusion and recrystallization phenomena at the interfaces of crystalline domains are expected during a process of surface compression.

Aggregation Structure of the Monomeric LB Film. Figure 4 shows the variation of transfer ratio during dipping cycles at surface pressures of (A) 18, (B) 25, and (C) 35 mN·m^{-1}. In this figure, "down" and "up" indicate downward dipping and upward drawing, respectively. White and black bars also indicate monolayer transferring and stripping, respectively. At a surface pressure of 35 mN·m^{-1}

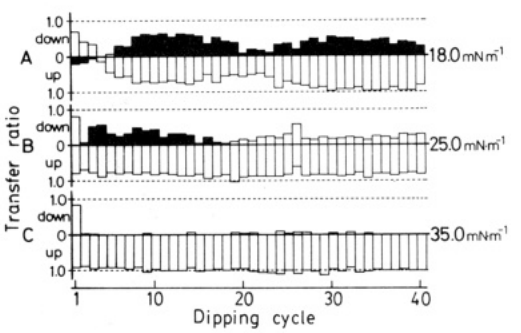

Figure 4. Variation of transfer ratio during dipping cycles at (A) 18, (B) 25, and (C) 35 mN·m^{-1}. (Down) downward dipping; (up) upward dipping; (white bar) monolayer transferring; (black bar) monolayer stripping.

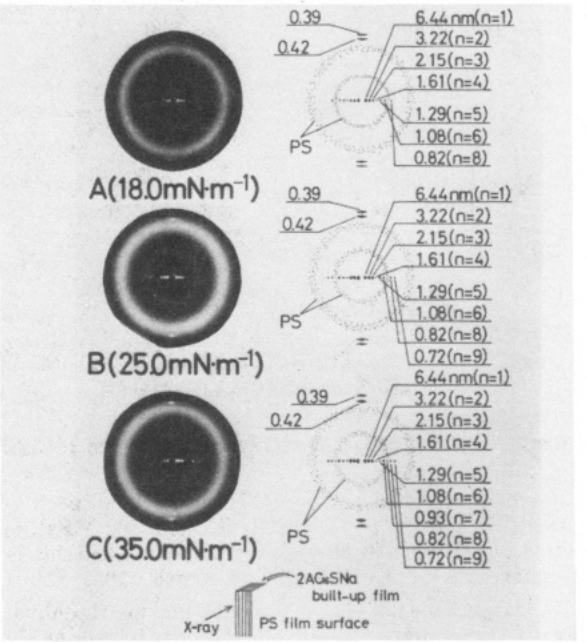

Figure 5. Wide-angle and small-angle X-ray patterns of LB films prepared at (A) 18, (B) 25, and (C) 35 mN·m^{-1} and their schematic representations.

(C), monolayers were transferred with a transfer ratio of 1 only during upward drawing. This is the typical dipping cycle of the Z-type LB film. It seems to be reasonable to conclude from the bright field image of Figure 3 and the transfer behavior of Figure 4C that the morphology of monolayer at 35 mN·m^{-1} is most homogeneous.

Figure 5 shows the wide- and small-angle X-ray patterns of the LB films prepared on polystyrene films at surface pressures of (A) 18, (B) 25, and (C) 35 mN·m^{-1} and their schematic representations. The incident X-ray beam was parallel to the film surface as shown in the lower part of Figure 5. In the X-ray scattering pattern of the LB film prepared at a surface pressure of 35 mN·m^{-1} (C), sharp scattering spots corresponding to a long spacing of 6.4 nm were observed on the equator up to the ninth order. The magnitude of the long spacing corresponded to a bimolecular length of $2AC_{16}SNa$, which apparently indicated that the Z-type LB film converted to the Y-type LB film. The sharp diffractions corresponding to the intermolecular distance among alkyl chains (0.39 and 0.42 nm) were observed on the meridian. Therefore, it is apparent from Figure 5 that the built-up layers are parallel to the film surface and in each built-up layer and the molecular axis is oriented perpendicular to the surface of built-up layer. Also, in the case of the LB films built up at (A) 18 and (B) 25 mN·m^{-1}, similar bilayer–lamella stacking to that at 35

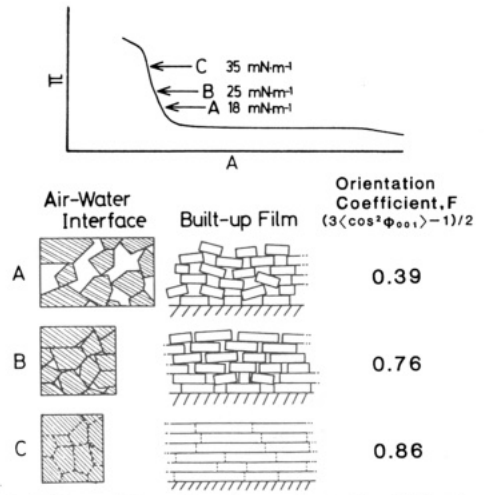

Figure 6. Values of lamella–plane orientation (right-hand side) and schematic representations of aggregation structures of monolayer (left-hand side) and LB film (middle) at (A) 18, (B) 25, and (C) 35 m·Nm^{-1}.

mN·m^{-1} was recognized. The magnitudes of the intermolecular spacings were independent of the built-up surface pressures. This indicates that the LB films have the same crystalline structures even though the built-up pressures are different.

To evaluate the degree of the lamella–plane orientation in the LB film prepared at various built-up pressures, small-angle X-ray scattering (SAXS) corresponding to the long period of the lamella–plane in the LB film was used. The orientation coefficient F was calculated from the X-ray intensity distribution along the azimuthal angle, Φ_{001}, by using the SAXS spot observed at $2\theta_B = 1.60°$ (Bragg angle). The following equation was used to calculate the magnitude of F:

$$F = {}^1/_2(3\langle\cos^2\Phi_{001}\rangle - 1)$$
$$= {}^1/_2\left(3\frac{\int_0^{\pi/2} I(\Phi_{001})\sin\Phi_{001}\cos^2\Phi_{001}\,d\Phi_{001}}{\int_0^{\pi/2} I(\Phi_{001})\sin\Phi_{001}\,d\Phi_{001}} - 1\right)$$

Here, $I(\Phi_{001})$ is the X-ray intensity at Φ_{001} corrected for background scattering. The values of F are 1.0 and 0.0, when lamella–planes orient perfectly parallel to the substrate surface and randomly, respectively. Figure 6 shows the value of F (right-hand side) and the schematic representations of the aggregation structures of monolayer (left-hand side) and LB films (middle) at (A) 18, (B) 25, and (C) 35 mN·m^{-1}. The schematic aggregation structure of monolayer can be concluded from the results of TEM observation (Figure 3). The value of F increased and became closer to 1.0 with an increase of the built-up pressure, indicating that the direction of normal vector of each lamella–plane became more uniformly perpendicular to the substrate surface. The monolayer film is composed of densely packed two-dimensional crystalline domains at 35 mN·m^{-1}, resulting in the formation of a morphologically homogeneous monolayer. On the other hand, it is expected that there are a lot of vacancies in the monolayer films at 18 and 25 mN·m^{-1}. In the middle of Figure 6, the aggregation structures of LB films prepared from the monolayer films with heterogeneous (18 and 25 mN·m^{-1}) and homogeneous (35 mN·m^{-1}) morphologies are schematically represented. In the case of the LB film prepared from heterogeneous monolayer films (18 and 25 mN·m^{-1}), the crystalline monolayer domains covering the second built-up layer dropped into the vacant or fractured portion which exists in the heterogeneous monolayer. Therefore, it is reasonably expected that the degree of lamella–plane orientation is low and the outermost surface of the LB film is morphologically rough, as shown in the middle of Figure 6. On the other hand, the LB film prepared from homogeneous monolayers at 35 mN·m^{-1} has a higher degree of lamella–plane orientation and the morphologically smooth outermost surface. From the results mentioned in Figures 3–6, it is apparently concluded that the optimum surface pressure for the preparation of the LB film with smooth outermost surface as well as the excellent lamella–plane orientation is 35 mN·m^{-1} in the case of $2AC_{16}SNa$.

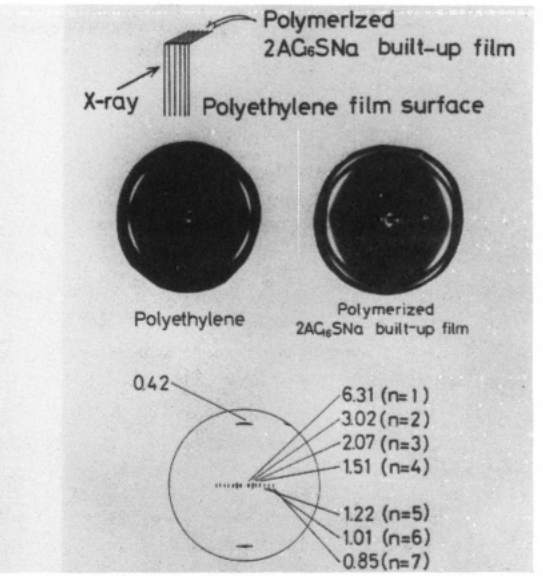

Figure 7. Wide-angle and small-angle X-ray patterns of polymerized LB films and their schematic representation.

Photopolymerization of the $2AC_{16}SNa$ LB Film. $2AC_{16}SNa$ monomeric LB films prepared on the polyethylene film were polymerized by UV irradiations. The completion of the polymerization reaction of LB film was confirmed by the disappearance of the C=C stretching bands (1640 cm^{-1}) and the C—H in-plane (1420 cm^{-1}) and out-of-plane (803 cm^{-1}) deformation vibration bands from the H_2C=CH– group on the basis of ATR-FT-IR measurements. The degree of polymerization was estimated to be 330 from gel permeation chromatography carried out with the chloroform solution of polymerized LB film. Figure 7 shows the wide- and small-angle X-ray patterns of the polymerized LB film and their schematic representation. The incident X-ray beam was parallel to the film surface as shown in the upper part of Figure 7. In the case of the polymerized LB film, the sharp diffractions corresponding to a long spacing of 6.3 nm were observed up to the seventh order on the equator. Diffractions corresponding to the intermolecular distance of 0.42 nm among alkyl chains were observed as arcs on the meridian. Though the long spacing was contracted at the value of 0.1 nm after polymerization in comparison with that in Figure 5, the highly oriented bilayer structure was preserved even after polymerization.

Surface Stability of the $2AC_{16}SNa$ LB Film. The stability in dried atmosphere of the hydrophilic surface of the LB film that was polymerized in water was investigated by angular dependent X-ray photoelectron spectra (XPS) measurement. Figure 8 shows the take-off angle (θ) dependence of the ratio of the number of sulfur to carbon atoms (S/C) for the monomer LB film and the LB film polymerized in water. Since the analyzing depth of XPS measurement is proportional to sin θ, the depth

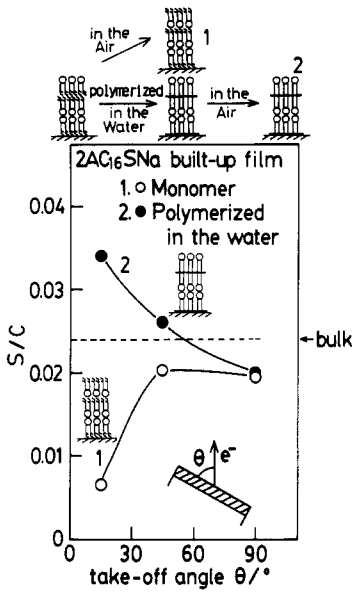

Figure 8. Take-off angle (θ) dependence of the ratio of S/C for the monomeric LB film and the LB film polymerized in water.

profile of elements in a shallower region from the outermost surface can be detected with a decrease in the take-off angle. The "bulk" in Figure 8 indicates the S/C calculated from the elemental composition of the $2AC_{16}SNa$ molecule. In the case of monomeric LB film (1, monomer), the magnitude of S/C decreased with a decrease in take-off angle and that of S/C at the take-off angle of 15° was much smaller than the calculated bulk value. This indicates that the surface of monomeric LB film is covered with hydrophobic parts of $2AC_{16}SNa$ to minimize the interfacial free energy in dried atmosphere, because the sulfur atom is in the hydrophilic part of $2AC_{16}SNa$. On the other hand, in the case of the LB film polymerized in water (2, polymerized in the water), the magnitude of S/C increased with a decrease in take-off angle and the S/C at 15° was much larger than the bulk value. This indicates that hydrophilic parts are maintained on the film surface of LB film even in dried atmosphere. Therefore, it is apparent that the hydrophilic surface of LB film is stabilized by polymerization in water. This may confirm that the overturning of monolayer at the outermost surface is reduced by a remarkable degree of polymerization or interlayer polymerization as shown in Figure 1B.

The stability of the hydrophobic surface of LB film that was polymerized in air was investigated by contact angle measurements in water. Figure 9 shows the variations of underwater surface–air–water contact angles (ϕ) with time immersed in water for the monomeric LB film, the LB film polymerized in air, and the LB film polymerized in water. To obtain the immobilized hydrophobic surface, the LB film was polymerized in air (2, polymerized in air). Though the monomeric LB film (1, monomer) showed overturning to the hydrophilic surface immediately after immersion in the water, the LB film polymerized in air (2, polymerized in air) stably maintained the hydrophobic surface for a long time even in the water. This result indicates that the external molecular assembly on the top surface of LB film is immobilized by polymerization. In the case of the LB film orienting the hydrophobic part to the film surface, the outermost monolayer was not polymerized in the manner of interlayer polymerization as shown in Figure 1A. Therefore, the hydrophobic surface of the LB film was immobilized because the highly polymerized large-area domain in the outermost monolayer can hardly turn over compared with the monomeric

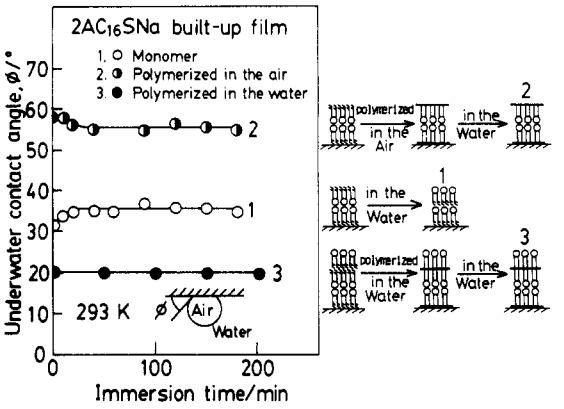

Figure 9. Variations of underwater surface–air–water contact angles (ϕ) with time immersed in water for the monomeric LB film and LB films polymerized in air and in water.

molecule. On the other hand, the LB film polymerized in water (3, polymerized in water) maintained its hydrophilic surface more stably for a long immersion time than the monomeric LB film.

Blood Compatibility of $2AC_{16}SNa$ LB Film. The blood compatibility was investigated as a surface functional property of the LB film. It is known that the inner wall of natural blood vessels is covered with the bilayer membranes of lipids and the surface is partially composed of mucopolysaccharides which possess anionic groups, such as sulfate and carboxylate groups.[8] It is supposed that this negative surface repels platelets and other blood components that are negatively charged. In addition, it is considered that heparin shows excellent antithrombogenicity because of the existence of sulfonic groups. Since $2AC_{16}SNa$ has a sulfonate in a hydrophilic part, the LB film orienting the hydrophilic part to the water–LB film interface is expected to show good blood compatibility. The degree of interaction between blood platelets and the surface of the LB film can be the measure for thrombogenicity of the LB film. Therefore, blood compatibility of the LB film was evaluated from the number of deformed platelets on the film surface. The morphology of adhered platelets on the substratum was classified into three types according to the degree of deformation:[2,3] (I) attachment of platelets at a point of contact with the substratum; (II) centrifugal growth of filopodia; (III) crytoplasmic webbing and flattening of the central mass. Since platelets of types II and III strongly adhere to the substrate, the number of adhered platelets of these types (number of deformed platelets) would be an index of thrombogenicity. Figure 10 shows the number of deformed platelets on the polymerized LB films with the hydrophobic and the hydrophilic surfaces, as well as monomeric LB film, glass plate, and original polyethylene film as reference materials. The polymerized LB film with a hydrophilic surface showed an excellent blood compatibility in comparison with other films, especially the polymerized LB film with a hydrophobic surface, indicating the weak interaction between the hydrophilic surface of the $2AC_{16}SNa$ LB film and the surface of platelets. Since $2AC_{16}SNa$ had a sulfonate in its hydrophilic part, the hydrophilic surface of the polymerized LB film was negatively charged. The good blood compatibility of the polymerized LB film with the hydrophilic surface is possibly attributed to the weak interaction between the negatively charged surface of platelets and the negatively charged surface of the LB films.

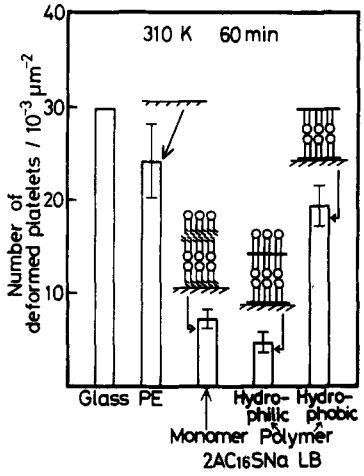

Figure 10. Number of deformed platelets on the polymerized LB films with the hydrophobic surface and with the hydrophilic surface and monomeric LB film showing the cases of glass and original polyethylene film as reference materials.

Conclusions

The LB film composed of a new amphiphile with a sodium sulfonate and two polymerizable alkyl chains had the bilayer lamella structure in which the lamella-plane oriented parallel to the film surface with the highest value of orientation coefficient, when it was prepared at the surface pressure at which the morphologically homogeneous monolayer film was formed on the water surface. The hydrophilic and hydrophobic surfaces of LB film were immobilized by polymerization carried out in water and in air, respectively. This is due to the progression of interlayer and/or intramonolayer polymerizations in LB film, preventing overturning of the outermost monolayer by a decrease in mobility of monolayer. When the interlayer polymerization progresses, the surface chemical structure does not change even if the overturning occurs. Therefore, the hydrophilic surface in air and the hydrophobic surface in water are immobilized, even though they are in thermodynamically unstable conditions. An excellent blood compatibility was observed for the polymerized LB film with a negatively charged surface.

References and Notes

(1) Lyman, D. J.; Knutson, K.; McNeil, B.; Shibatani, K. *Trans.—Am. Soc. Artif. Intern. Organs* **1975**, *21*, 49.
(2) Takahara, A.; Tashita, J.; Kajiyama, T.; Takayanagi, M. *Kobunshi Ronbunshu* **1982**, *39*, 203.
(3) Takahara, A.; Tashita, J.; Kajiyama, T.; Takayanagi, M.; MacKnight, W. J. *Polymer* **1985**, *26*, 978.
(4) Takahara, A.; Tashita, J.; Kajiyama, T.; Takayanagi, M.; MacKnight, W. J. *Polymer* **1985**, *26*, 987.
(5) Takahara, A.; Tashita, J.; Kajiyama, T.; Takayanagi, M. *J. Biomed. Mater. Res.* **1985**, *19*, 13.
(6) Takahara, A.; Jo, N.-J.; Kajiyama, T. *J. Biomater. Sci., Polym. Ed.* **1989**, *1*, 17.
(7) Ward, R. S.; White, K. A.; Hu, C. B. In *Polyurethanes in Biomedical Engineering*; Planck, H., Egbers, G., Syre, I., Eds.; Elsevier: Amsterdam, 1984; p 181.
(8) Sawyer, P. N.; Burrowes, C.; Ogoniak, J.; Smith, A. O.; Wesolowski, S. A. *Trans.—Am. Soc. Artif. Intern. Organs* **1964**, *10*, 316.
(9) Blodgett, K. B. *J. Am. Chem. Soc.* **1935**, *57*, 1007.
(10) Oda, T.; Takahara, A.; Uchida, M.; Kajiyama, T. *J. Chem. Soc. Jpn.* **1987**, *1987*, 2163.
(11) Uchida, M.; Tanizaki, T.; Kunitake, T.; Kajiyama, T. *Macromolecules* **1989**, *22*, 2381.
(12) Fereshtehkhou, S.; Neuman, R. D.; Ovalle, R. *J. Colloid Interface Sci.* **1986**, *109*, 385.
(13) Fukuda, K.; Nakahara, H.; Kato, T. *J. Colloid Interface Sci.* **1976**, *54*, 430.
(14) Andrade, J. D.; King, R. N.; Gregonis, D. E.; Coleman, D. L. *J. Polym. Symp.* **1979**, *66*, 313.
(15) Ishikawa, J.; Uchida, M.; Oishi, Y.; Kajiyama, T. *Rep. Prog. Polym. Phys. Jpn.* **1990**, *33*, 235.
(16) Tieke, B.; Wiess, K. *J. Colloid Interface Sci.* **1984**, *101*, 129.
(17) Dutta, P.; Peng, J. B.; Lin, B.; Ketterson, J. B.; Prakash, M.; Georgopoulos, P.; Ehrlich, S. *Phys. Rev. Lett.* **1987**, *58*, 2228.
(18) Kajaer, K.; Als-Nielsen, J.; Helm, C. A.; Tippman-Krayer, P.; Möhwald, H. *J. Phys. Chem.* **1989**, *93*, 3200.
(19) Uyeda, N.; Takenaka, T.; Aoyama, K.; Matsumoto, M.; Fujiyoshi, Y. *Nature* **1987**, *327*, 319.
(20) Kajiyama, T.; Umemura, K.; Uchida, M.; Oishi, Y.; Takei, R. *Bull. Chem. Soc. Jpn.* **1989**, *62*, 3004.
(21) Kajiyama, T.; Tanimoto, Y.; Uchida, M.; Oishi, Y.; Takei, R. *Chem. Lett.* **1989**, *1989*, 189.
(22) Kajiyama, T.; Morotomi, N.; Uchida, M.; Oishi, Y. *Chem. Lett.* **1989**, *1989*, 1047.

Registry No. 1, 133495-49-5; 2, 133495-50-8; $2AC_{16}SNa$, 112360-11-9; $2AC_{16}SNa$ polymer, 133495-51-9; maleic anhydride, 108-31-6; 1,16-hexadecanediol, 7735-42-4; acryloyl chloride, 814-68-6.